MODELLING AND OPTIMIZATION OF A LASER DROPLET-FORMATION PROCESS

MODELIRANJE IN OPTIMIZACIJA LASERSKEGA TVORJENJA KAPLJICE

Tadej Kokalj[1], Igor Grabec[2], Edvard Govekar[2]

[1]Institute of Metals and Technology, Lepi pot 11, 1000 Ljubljana, Slovenia
[2]Faculty of Mechanical Engineering, University of Ljubljana, Aškerčeva 6, 1000 Ljubljana, Slovenia
tadej.kokalj@imt.si

The laser droplet-formation process (LDFP) is a part of the novel joining technology for forming high-temperature joints. The advantages of this technology are: good heat-input control, good control of the added material and limited local heating. A molten metal droplet is used as the basic unit for the filling material, and a determination of the process parameters for the formation of droplets with desired properties is crucial. A physical and numerical model of the process was built to allow a theoretical determination of the process parameters. The numerical model enables a simulation of the process at different sets of parameters and a genetic algorithm optimization was implemented to find the best set. To verify this general procedure for determination and optimization of the parameters, we applied it in a specific case of a nickel wire. On the basis of the numerical model of the process, laser pulses for pendant-droplet formation and droplet detachment were determined and applied in experiments. With numerically determined laser pulses pendant-droplet formation and detachment were accomplished. In most cases, the process showed a very high repeatability. The encouraging experimental verification shows that a numerical approach is a very helpful tool for a determination of the process parameters and a better understanding of the process. It significantly reduces the number of necessary experiments when the laser droplet-formation setup or the target droplet properties are changed.

Keywords: droplet formation, laser, modelling, optimization, experimental verification

Proces laserskega tvorjenja kapljice (LTK) je del nove tehnologije spajanja za tvorjenje visokotemperaturnih spojev. Prednosti te tehnologije so: dobra kontrola vnesene toplote in dodanega materiala ter omejeno lokalno segrevanje podlage. Staljena kovinska kapljica se uporabi kot dodajni material, parametri za tvorjenje kapljice s primernimi lastnostmi pa so bistveni za uspešnost procesa. Zgradili smo fizikalni in numerični model procesa, ki omogoča teoretično določitev optimalnih procesnih parametrov. Numerični model omogoča simulacijo procesa pri različnih naborih parametrov, optimizacijo z genetskimi algoritmi pa smo uporabili za iskanje najboljšega nabora. Za eksperimentalno potrditev tega splošnega načina smo metodo uporabili v konkretnem primeru nikljeve žice. Na osnovi teoretičnega modela smo določili laserski blisk za tvorjenje in odlet kapljice ter jih uporabili v poskusih. Z numerično določenimi laserskimi bliski smo uspešno tvorili in ločili kapljico od žice. V večini primerov je proces izredno dobro ponovljiv. Uspešna eksperimentalna potrditev potrjuje pomembnost teoretičnega modela za določitev procesnih parametrov in boljše razumevanje procesa. Numerični model močno zmanjša potrebno število eksperimentov za določitev procesnih parametrov ob spremembi vrste žice ali spremembi ciljnih lastnosti tvorjenih kapljic.

Ključne besede: tvorjenje kapljice, laser, modeliranje, optimizacija, eksperimentalna verifikacija

1 INTRODUCTION

A constant technological advance is increasing the demand for joining new and dissimilar materials, for which conventional technologies are neither appropriate nor convenient. The differences in the thermophysical properties of base materials and the trend of miniaturisation require a better control of the heat input and the amount of a filler material. In order to improve this control, droplet-joining technologies are investigated where a small, molten metal droplet is used as the basic unit of a filling material. The droplet is deposited on a joining spot creating a material-to-material joint or a bridge over a gap in the substrate.[1,2]

Several droplet-formation technologies have been proposed for the applications in the joining technologies. Individual droplets are generated by different "drop-on-demand" generators.[3–5] In the case of low-melting materials (300 °C to 500 °C), the melted material is provided from a heated reservoir. A droplet is then generated with a short pressure pulse.[5,6] Produced joints are not susceptible to high temperatures and usually contain lead that is environmentally disputable. The generation of droplets from a high-melting material (typically over 1000 °C), is usually accomplished with local heating of a wire. The first systems for droplet generation used a pulsed electric arc between the electrodes and the tip of the wire.[7–9] A molten metal droplet was then detached from the wire by the electromagnetic force, as a consequence of an increase in the electric current at the end of the pulse[10,11], which could be accompanied by mechanical oscillations of the wire.[12] The diameter of a droplet in this technology is limited down to 1 mm.[13] A system for the arc-droplet formation does not allow for a precise energy control. Besides, an electric arc induces the formation of hot plasma, which strongly heats the surroundings. The system has to be intensely cooled and it is not appropriate in the cases when the heat susceptibility of the substrate is limited.

To avoid the listed deficiencies of the formation of high-temperature joints, a new laser droplet-formation technology was proposed.[14,15] In this novel technology a laser beam is used for droplet formation and detachment from the feed wire (**Figure 1**). The advantage of this technology is a good heat-input control and limited local heating enabling a formation of smaller droplets.[15–17]

The laser droplet-formation process (LDFP) was proposed as part of a new droplet-joining technology in[15] and was first characterized with an IR camera and acoustic emission signals in[14]. A detailed characterization of the process on the basis of acoustic emission, where different phases of the process such as heating, melting, droplet formation and droplet detachment are observed, is given in[18]. A possibility of an indirect process characterization by means of reflected laser light is explained in[16]. The cooling of a droplet after its detachment and examples of blind joints are discussed in[17] and an application for joining the parts of different materials and geometrical properties are elaborated in[19]. Later a sequential formation of droplets was presented and the chaotic regimes of sequential-droplet formations were elaborated and discussed in[20]. Lately, some promising studies were done on the application of droplet welding of coated steel sheets.[21]

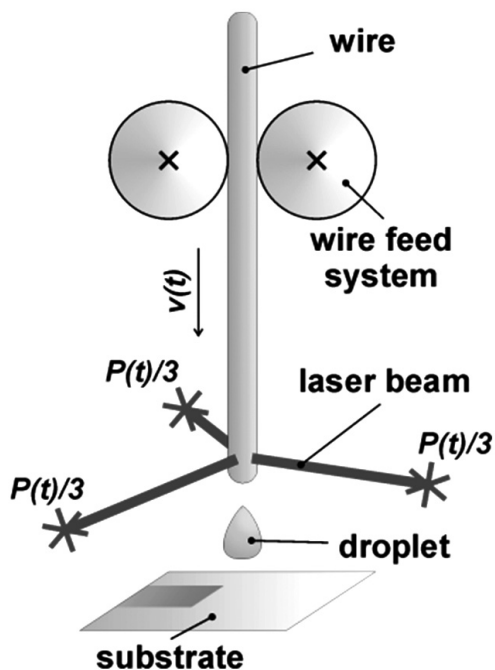Determining the process parameters, especially the time course of the laser power, proves to be of the central importance for the repeatable formation of droplets with desired properties. The first experimental investigations showed that it is difficult to achieve a repeatability of the process and to avoid undesired radial scatter and splashing of the melt by the heuristically determined laser pulses. At the beginning, a laser pulse of a constant power was used with a steel wire, however, the time course of the laser power and velocity of the wire movement were later identified to be the most important process parameters. A simple theoretical analysis of the process[22] as well as the experimental results showed that it is convenient to divide LDFP into two phases: the pendant droplet formation and the detachment phase. With this approach the process was significantly improved. However, in order to further improve the control of droplet properties, like the size, temperature homogeneity and heat content, and to avoid undesired splashes, a numerical model of the process was built.

The numerical model enables the simulation of the process at different sets of process parameters. With the use of the numerical model and genetic-algorithm optimization method, the process parameters can be optimized in accordance with the selected optimization objectives. These optimization objectives incorporate the desired droplet properties corresponding to the purpose of an application. The theoretical approach showed to be very useful not only to get a better insight into the process, but especially as a general tool to significantly decrease the number of the experiments needed to find new process parameters when some of the parameters are changed (i.e., wire material or diameter, laser optics, wire velocity, etc.).

The article starts with a description of the physical and numerical model of the process. An application of genetic algorithms for determining the pendant-droplet-formation pulse is described together with the applied objective functions. At the end of the theoretical part of the paper the procedure for determining the droplet-detachment pulse is explained on the basis of a simplified model of the keyhole phenomenon. In the second part of the paper we focus on the experimental verification of theoretical results. The laser droplet-formation process is explained for a specific case of a nickel wire. The results of the theoretical treatment with determined laser pulses and the corresponding simulations are presented in parallel with the experimental results for both pendant-droplet formation and detachment of a droplet. In the last section we discuss the results and underline the significance of this research for a further development of the process.

Figure 1: In the laser droplet-formation process (LDFP) a thin metal wire is fed to the focus of laser beams. A hot molten droplet is formed at the tip of the wire, detached by a sudden increase in the laser power and deposited on the substrate.
Slika 1: Pri laserskem tvorjenju kapljice (LTK) dodajamo tanko kovinsko žico v gorišče laserskih žarkov. Vročo staljeno kapljico, ki nastane na koncu žice, ločimo s kratkotrajnim povečanjem laserske moči. Kapljica pade na podlago, kjer tvori spoj.

2 THEORETICAL MODEL AND NUMERICAL MODEL

With the aim of theoretically determining the laser pulse, a numerical model of the process was built. The basic equation of this model is the heat equation in cylindrical coordinates (r, ϑ, z):

$$\frac{\partial T(r,\vartheta,z,t)}{\partial t} = D(T)\left[\frac{1}{r}\frac{\partial}{\partial r}\left(r\frac{\partial T(r,\vartheta,z,t)}{\partial r}\right)+\right.$$
$$\left.+\frac{1}{r^2}\frac{\partial^2 T(r,\vartheta,z,t)}{\partial\vartheta^2}+\frac{\partial^2 T(r,\vartheta,z,t)}{\partial z^2}\right] \quad (1)$$

where T is the temperature and $D(T) = k(T)/\rho(T)c_p(T)$ is the temperature-dependant heat-diffusion coefficient. In this equation the temperature-dependent gradient of the heat-conduction coefficient k was neglected.

Phase transitions were treated as jumps in specific heat:

$$c_{pt}(T) = c_p(T) + L\delta(T - T_p) \quad (2)$$

where c_{pt} is the total specific heat, including the latent heat L, c_p is the specific heat at the instant temperature, δ is the Dirac delta function and T_p is the temperature of the phase transition. For the numerical approximation of δ, a Gaussian function was used:

$$\delta(T - T_p) \approx \frac{1}{\sqrt{2\pi}\Delta T}\exp\left(-\frac{(T - T_p)^2}{2\Delta T^2}\right) \quad (3)$$

Here ΔT is the adaptable width of the Gaussian function.

The temperature of the wire at the beginning of the process is the same as the environmental temperature T_0, therefore we formulate the initial condition as:

$$T(\vec{r},0) = T_0 \quad (4)$$

With respect to the boundary conditions we consider the thermal radiation from the hot surface as:

$$j_r(\vec{r}_{sur},t) = -\sigma T^4 \quad (5)$$

Since the radiation flux from the wire is much larger than the radiation flux from the environment to the wire, the latter is neglected in this formulation.

The energy flux of the laser beams to the wire is a function of the spatial part $j_l(\vec{r})$, the temporal part $g(t)$ and it depends on the material absorptivity A:

$$j_f(\vec{r}_{sur},t) = Aj_l(\vec{r})g(t) \quad (6)$$

The boundary condition on the surface of the wire is finally formulated as:

$$k(T)\frac{\partial T}{\partial n} = j_f - j_r \quad (7)$$

where k is the thermal conductivity and $\partial T/\partial n$ is the temperature gradient in the direction perpendicular to the surface. The sum of thermal fluxes is on the right-hand side of the equation.

The heat equation including the described initial and boundary conditions can be solved numerically using an explicit finite-difference scheme in cylindrical coordinates.[23] With the described numerical model the time development of the temperature field of the wire at various sets of process parameters can be simulated. Based on the simulations a proper set of process parameters can be determined and optimized. This work is focused on determining the laser pulse.

3 LASER-PULSE DETERMINATION

The laser pulse for pendant-droplet formation and the pulse for droplet detachment were determined separately. In the first part of the process the heat input is essential and in the second part a sufficient force is needed to detach the droplet. Although both parts of the process are coupled, we treated them separately for the sake of simplicity. The pendant-droplet-formation pulse was parameterized with seven parameters (**Figure 2**) and these were subject to optimization. The droplet-detachment pulse was determined on the basis of a simplified keyhole-effect model. We need to stress that only the parameterized laser pulse was optimized in this investigation, while the other parameters were pre-selected by selecting the wire, limiting our experimental setup and the desired size of the droplet and were not subject to optimization. However, the described optimization procedure can also be used to optimize other parameters.

3.1 Laser pulse for pendant-droplet formation

In the pendant-droplet-formation phase of the process, a well-melted pendant droplet has to be produced at the tip of the wire. Besides, the splashing of the melt and the radial scatter of deposited droplets have to be reduced. Since the droplet properties (i.e., heat content and temperature homogeneity) are importantly influenced in this part of the process, the laser pulse should be determined in accordance with the desired droplet properties.

The selection of a proper method for laser-pulse determination depends on the time necessary for one
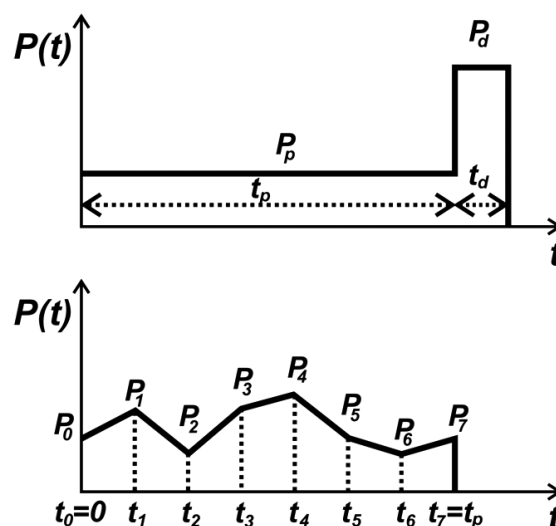
Figure 2: Simple laser pulse for LDFP consists of two parts: pendant-droplet-formation part and detachment part (top). In the present work we parameterized the first part of the pulse with seven parameters in order to further optimize the heat input (bottom).
Slika 2: Enostaven laserski blisk za LTK je sestavljen iz dveh delov: del za tvorjenje viseče pretaljene kapljice in del za ločitev kapljice (zgoraj). V predstavljenem delu smo prvi del bliska parametrizirali s sedmimi parametri za nadaljno optimizacijo vnosa toplote (spodaj).

process simulation. The numerical model was implemented in the C++ language. It is basically 3D and can be used either for a 2D or 3D simulation of the process. An increased spatial dimensionality of the model drastically increases the simulation time, therefore, the dimensionality of the problem is reduced. Since three laser beams are positioned equidistantly around the circumference of the wire, and the diameter of the laser beam is similar to the wire radius, the process can be considered as quasi-symmetrical. In this ax-symmetrical case the angular dependence can be abandoned and a 2D model is sufficient to describe the process.

A short simulation time allows an implementation of the optimization method that requires many process simulations. We choose the genetic-algorithm method[24-26] for the process optimization.

To perform the optimization, we need to determine the fitness function that includes the objectives of the optimization encoded in a single mathematical expression. We determined two different fitness functions. The first fitness function was assigned as:

$$J_1 = 1 - \frac{m_t}{m} + \frac{m_i}{m} \qquad (8)$$

where m_t/m is the portion of the melted material, and m_i/m is the portion of the vaporized material. The objective of this function is to get the highest possible amount of the melted material at the lowest possible vaporization. By finding the minimum of this function, we achieve the best trade-off between the amounts of the melted and vaporized material at the end of a laser pulse.

The second fitness function is more complex and composed of two parts:

$$J_2 = \frac{1}{2} \frac{\sqrt{\sum_{j=1}^{N} (T_j(t_v) - T_z)^2 \cdot \frac{m_j}{m_D}}}{T_z} + \frac{1}{2} \cdot \frac{1}{M} \sum_{k=1}^{M} \frac{m_{ik}(t_k)}{m_D} \qquad (9)$$

where $T_j(t_v)$ is the temperature of the j-th volume part of the wire at the time t_v and m_j is its mass; m_D is the mass of the observed part of the wire and T_z is the desired final temperature of the wire; m_{ik} is the mass of the vaporized material at the time t_k.

The first part of the fitness function is calculated at the end of the laser pulse t_v and should bring the final temperature of the wire as close to the desired temperature T_z as possible. The role of the second part of the fitness function is to prevent vaporization during the pulse. It is calculated as the sum of the portions of the vaporized material at the $M = 100$ intervals from the beginning, $t = 0$, to the end of the laser pulse, $t = t_v$.

With these two fitness functions and the selection of desired temperatures T_z, different laser pulses for pendant-droplet formation were determined. In addition, the arbitrary-fitness function can be constructed in order to meet the demand of a specific application. The optimization was performed by combining the executable

C++ file, the returning value of the fitness function at the selected set of parameters and MATLAB Genetic Algorithm Toolbox, creating a new set of parameters. The time for the optimization of one laser pulse was around 20 h including several hundred process simulations.

3.2 Laser pulse for droplet detachment

After a successful formation of a pendant droplet at the tip of the wire an additional force is needed to overcome the surface tension force[20] and detach the droplet from the wire. This additional force is provided by an onset of the keyhole. The keyhole is a highly nonlinear phenomenon and therefore difficult to model, particularly in the first transient phase when the keyhole is being formed. Since the numerical model of the transient phase of the keyhole effect was not found in the literature, we built a simplified numerical model of this part of the process. We treated the keyhole as a fast vaporization of the material and we neglected the self-focusing dynamics of the keyhole due to the surface tension. In this way we could approximately simulate the growth of the keyhole.

It was shown in[22] that a droplet can be detached from the wire when the depth of the keyhole approximately reaches the axes of the wire. Therefore, the droplet-detachment pulse was determined in the following way: First, a constant laser power was selected for the laser pulse. Second, the time development of the temperature field was calculated for the selected laser power and the temperature on the axis of the wire was checked on each time step. Third, the calculation was stopped when the temperature on the axis of the wire reached the boiling temperature, that is when the keyhole reached the axis of the wire.

With this procedure the necessary time to form a keyhole and detach the droplet from the wire, or better, its upper limit, was determined since the keyhole growth, considering the self-focusing, was even faster. It is important to minimize the detachment-pulse time in order to reduce the unnecessary heating of the wire with the high-power laser beam, resulting in undesired effects like vaporization and splashes of the melt.

4 EXPERIMENTS AND RESULTS

The theoretical model, pulse determination and optimization procedure described above are general and independent of the wire, laser and wire-feed unit. However, in order to evaluate the adequacy of theoretical work, we determined the laser pulses and performed experiments for a specific case of a nickel wire of a diameter 0.7 mm using the experimental setup described below. The results of numerical calculations and experimental outcomes are described in the following section.

4.1 Experimental system

The main parts of the experimental system are: a laser, a wire-feed unit, an opto-mechanical positioning system and a measuring computer.

The heart of this system is a Nd:YAG pulse laser which operates at the wavelength of $\lambda = 1064$ nm. The maximum frequency of the laser-pulse generation is $\nu = 300$ Hz and the average power is $\bar{P} = 0.25$ kW. The minimum power of the laser pulse is $P_{min} = 0.48$ kW and the maximum laser power is $P_{max} = 8$ kW. The minimum and maximum durations of the laser pulse are $t_{min} = 0.3$ ms and $t_{max} = 20$ ms. The time course of the laser power of a pulse can be set with a time step of 0.1 ms and a power step of 40 W.

The wire-feed unit enables the maximum acceleration of the wire, $a_{max} = 20$ m/s^2, and the maximum velocity is $v_{max} = 0.3$ m/s. The step size of the wire move is $z_{min} = 3.1$ μm.

For the investigation of LDFP the primary laser beam is split into three laser beams of equal power. These laser beams are led by means of optic fibres to exit the opti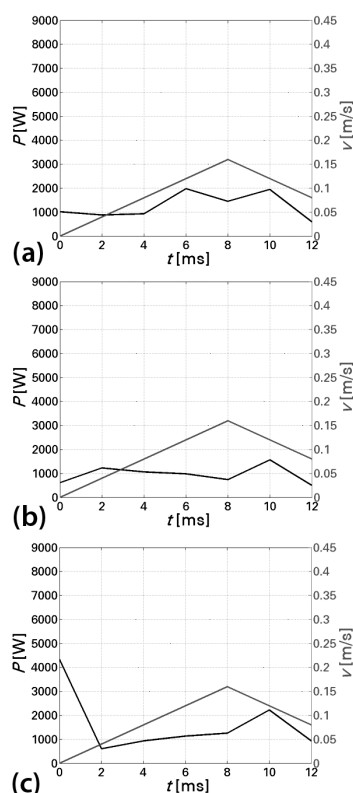cs of the laser. This optics is equidistantly positioned around the wire in the plane perpendicular to the wire. The focal length of the exit lens is $f = 100$ mm and the diameter of the laser beam in focus is $d_f = 0.4$ mm. For an easier positioning of the wire and monitoring of the process, the laser optics is equipped with the CCD cameras connected to the screens. Laser optics can be precisely positioned in accordance with the wire using a system of micrometer positioning stages.

4.2 Pendant-droplet formation

The laser droplet-formation process was separated into two phases. The first phase is the formation of a pendant droplet at the tip of the wire and the second phase is the detachment of the droplet from the wire. Therefore, we divided the total laser-pulse duration of 20 ms into a 12 ms part for the formation of the pendant droplet and the remaining 8 ms of the laser pulse for the droplet detachment.

First, the laser pulses for pendant-droplet formation were theoretically determined as described in section 3.1. Examples of the laser pulses are shown in **Figure 3**.
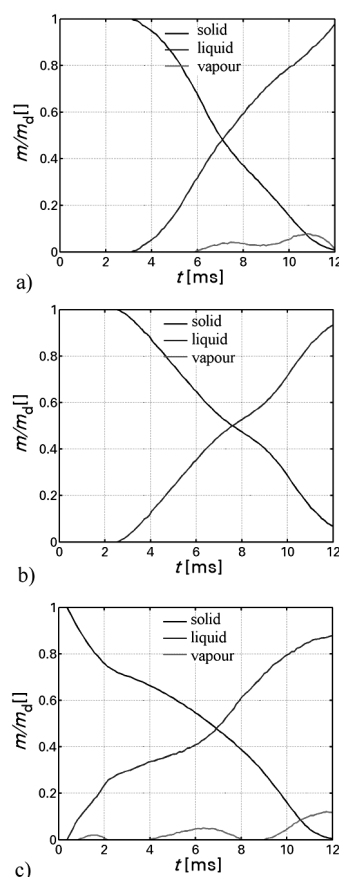

Figure 3: Examples of laser pulses (black line): a) laser pulse determined with the fitness function J_1 and laser pulses determined with the fitness function J_2 with the selected final temperatures: b) $T_{z1} = 2000$ K and c) $T_{z2} = 3000$ K. Grey line denotes the velocity profile of the wire movement.

Slika 3: Primeri laserskih bliskov (črna črta): a) laserski blisk, določen s kriterijsko funkcijo J_1 in laserska bliska, določena s kriterijsko funkcijo J_2 in različnimi ciljanimi končnimi temperaturami: b) $T_{z1} = 2000$ K in c) $T_{z2} = 3000$ K. Siva črta prikazuje hitrostni profil podajanja žice.

Figure 4: Time courses of the shares of the material in solid, liquid and vapour phases during the laser pulses. Graphs correspond to the laser pulses shown in **Figure 3**.

Slika 4: Časovni potek deleža materiala v trdnem, tekočem in plinastem stanju med trajanjem laserskega bliska. Slike po vrsti ustrezajo laserskim bliskom s **slike 3**.
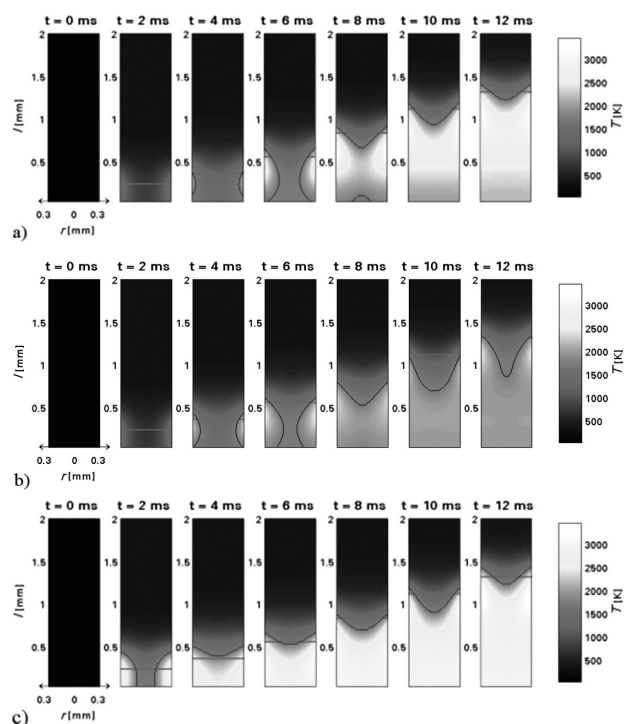
Figure 5: Evolution of the temperature field of the wire. Images correspond to the laser pulses shown in **Figure 3**.
Slika 5: Razvoj temperaturnega polja žice. Slike ustrezajo laserskim bliskom s **slike 3**.

The first pulse is determined with the fitness function J_1 that was used to assure the best trade-off between the shares of the melted and vaporized material. With the second J_2 fitness function we aimed at bringing the uniform temperature of the droplet as near to the desired temperature as possible. Besides, we wanted to decrease the vaporization of the material during the pendant-droplet formation, which was achieved with the second term in the fitness function. The first selected temperature is just above the melting temperature of nickel and the second is near the boiling temperature of nickel. The above-mentioned figure shows how the pulses differ, not just in the energy, but also in the time course of the laser power. At the beginning they differ a lot, but at the end they all have similar shapes. The laser power increases in the interval from 8 ms to 10 ms because the wire is moving with the largest velocity. At the end, when the velocity is decreased, the laser power is correspondingly reduced.

From the theoretical model we can also predict the share of the material in each phase during the laser-pulse duration, as shown in **Figure 4**.

As can be seen from the above figure, at the beginning, all material is in the solid phase. After a certain period the melting sets in. By the end of the pulse most of the material is melted and some of the material is vaporized. In the model vaporization is treated as the overheated liquid material that turns into a liquid if it cools down.

The evolution of the temperature field of a cross-section of the wire is shown in **Figure 5**.

The horizontal line denotes the position of laser beams and the black curves divide the material in different phases. The temperature fields can be compared to the experimental results. Three typical final states of the pendant droplet after solidification are shown in **Figure 6**.

The dashed cross in the image denotes the final position of the laser beam and the non-dashed cross was used for an easier positioning of the wire.

The first temperature field of the wire predicts the melted wire, but, as we can see in the photo, the tip of the wire is not completely melted. There is a knob on the wire tip that corresponds to the area of the lowest temperature predicted by our model. The core of the wire was probably not completely melted at the wire tip and the consequence is an irregular shape of the droplets.

As shown in the second figure of the temperature field, the predicted temperature of the wire tip is just above the melting temperature of nickel (1727 K). In the image of the experimental outcome we can see that no droplet was formed at the tip of the wire. The only noticeable effect of laser heating is a deformation of the wire at the position where the highest wire temperature is predicted by the model. This deformation is denoted with a white arrow in the image of the experimental outcome. The reason for a disagreement of the model prediction with the experimental results is the presumption on the uniform heating of the wire circumference, due to the simplification of the model.
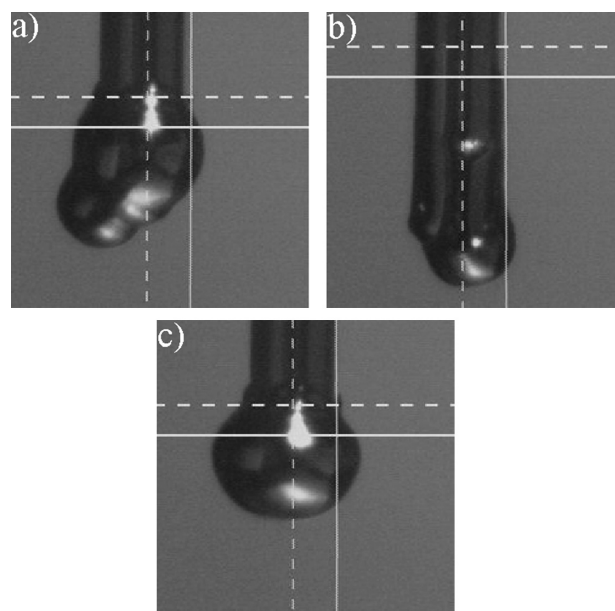

Figure 6: Typical examples of experimental outcomes of pendant-droplet formation. Droplets correspond to the laser pulses shown in **Figure 3** denoted with the same letters.
Slika 6: Tipični primeri eksperimentalnih tvorjenj viseče kapljice. Kapljice ustrezajo laserskim bliskom s **slike 3** in so označene z ustreznimi črkami.
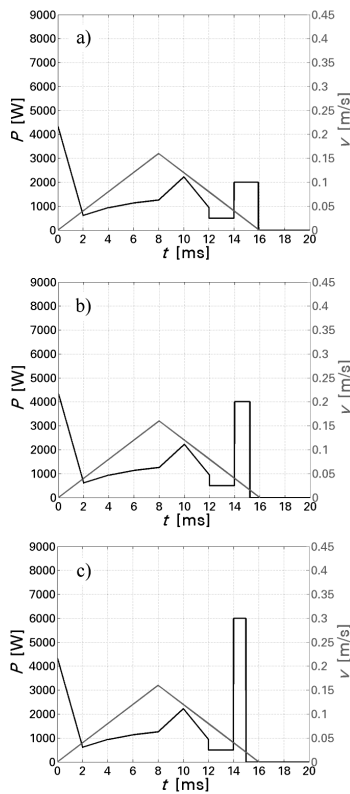
Figure 7: Three examples of laser pulses with the same pendant-droplet-formation parts and different detachment parts. Droplet-detachment pulses are of: a) 2000 W, b) 4000 W and c) 6000 W.
Slika 7: Trije primeri laserskih bliskov z enakim začetnim delom za tvorjenje viseče kapljice in različnimi bliski za ločitev kapljice. Bliski za ločitev kapljice imajo moči: a) 2000 W, b) 4000 W in c) 6000 W.

In the third case the model predicts a very hot tip of the wire near the boiling temperature. The experimental outcomes yield a repeatable formation of the melted droplets at the tip of the wire.

4.3 Droplet detachment

After the formation of a pendant droplet, we have to detach it from the wire. An additional high-intensity laser pulse is needed to assure a droplet detachment. This additional laser pulse is determined as described in section 3.2. The laser power is selected in advance and the duration of a laser pulse is determined in line with the requirement that the boiling temperature reaches the axis of the wire.

The best laser pulse for pendant-droplet formation was selected and a short time of 2 ms for the minimum laser power of $P_{min} = 480$ W was added to that pulse. This pause was heuristically introduced to allow a droplet relaxation, since the droplet oscillates after it is formed at the tip of the wire. Three examples of the calculated laser pulses are shown in **Figure 7**.

The required time for droplet detachment decreases with an increased laser power as expected. The dependence of the necessary pulse duration on the applied laser power is shown in **Figure 8**.
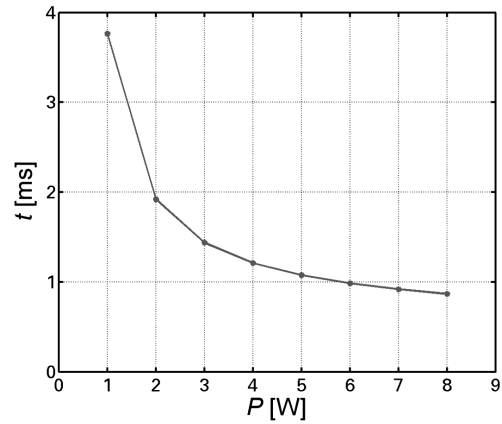

Figure 8: Dependence of detachment-pulse duration on the selected laser power
Slika 8: Odvisnost trajanja bliska za ločitev kapljice od izbrane moči laserja

The time development of the temperature field of the wire during a droplet-detachment pulse is shown in **Figure 9**.

The detachment pulse is stopped when the boiling temperature reaches the axis of the wire. The horizontal line denotes the position of the laser beams. The results of the model show that more material is melted when a higher laser power is used in spite of a shorter pulse time.

After the theoretical determination of detachment pulses, the experiments were performed for the evaluation of theoretical results. A laser pulse for a droplet detachment cannot be tested alone. Therefore, different detachment pulses were added after a relaxation period 2 ms that followed the same pendant-droplet-formation pulse.

With each laser pulse 10 droplets were produced and deposited on the substrate placed horizontally 3.5 mm below the focus of the laser beams. Examples of droplets are shown in **Figure 10**.

Radial scatter and a number of splashes on the substrate depend on the applied laser pulse. Droplets are systematically shifted to the left. The images of typical droplets in **Figure 10** show that the droplets differ also in the roughness of the contact region and the shape of a droplet on the substrate.
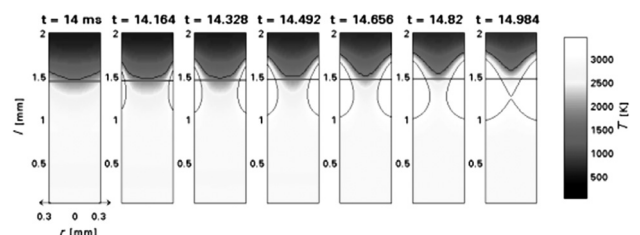

Figure 9: Time development of the temperature field during a droplet-detachment pulse
Slika 9: Časovni razvoj temperaturnega polja kapljice med bliskom za ločitev kapljice
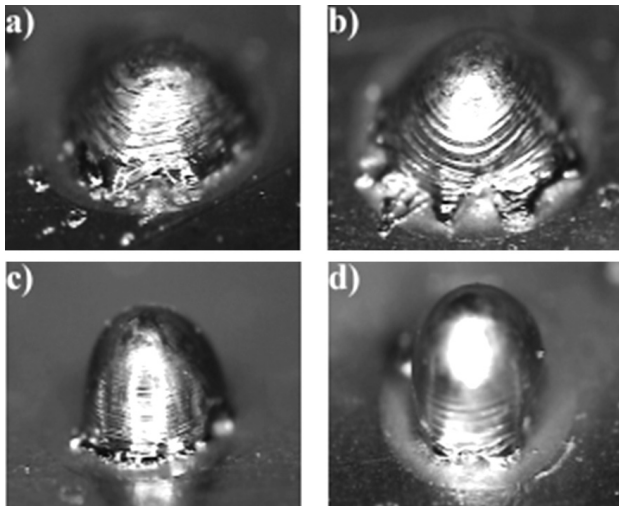
Figure 10: Magnifications of typical droplets from the sets produced with different detachment pulses
Slika 10: Povečava tipičnih kapljic iz zaporedij, tvorjenih z različnimi bliski za ločitev kapljice

For the purpose of evaluation and comparison a more detailed quantitative analysis of the experimental results was performed. The basic criterion for the successfulness of the process is the detachment of a droplet. Undesired splashes on the substrate were also counted. The repeatability of droplet deposition and droplet size was characterized with the size and standard deviation of these parameters. The results of the analysis are presented in **Table 1**.

We introduced variability of the process, V:

$$V = \frac{\sigma_d}{\bar{d}} + \frac{\sigma_r}{\bar{d}} \qquad (10)$$

where the standard deviation of the droplet diameter is $\sigma_d = \sqrt{\sigma_{dx}^2 + \sigma_{dy}^2}$, the standard deviation of the droplet position from the expected position is $\sigma_r = \sqrt{\sigma_{rx}^2 + \sigma_{ry}^2}$ and $\bar{d}$ is the average droplet diameter for a set. The ratio between the number of splashes on the substrate N_{izb} and the number of detached droplets in a set N_{kap} was calculated.

At the highest power of a detachment pulse, a droplet was always detached, but accompanied by numerous splashes. At a smaller laser power, droplets sometimes stay undetached. At a laser power of 2 kW droplets always stayed attached to the wire. At a laser power of 4 kW two droplets stayed undetached and at 5 kW one droplet stayed undetached. At a laser power of 6 kW all the droplets detached from the wire. Also, the variability of the process decreases with the laser power. The process variabilities at the laser powers of 4 kW, 5 kW and 6 kW are very similar.

5 DISCUSSION AND CONCLUSION

A laser droplet-formation process is discussed in the article. For the first time a more detailed physical and numerical model of the process is presented. After building an experimental system and conducting quite an extensive experimental work we find out that the process is very complex in a sense of a high number of influencing parameters and instable in a sense of the sensitivity to small parameter change. To get a deeper insight into the process we decided to build a more detailed theoretical and numerical model of the process. Instead of using the model just for the analysis of the process we decided to determine certain selected process parameters on the basis of a numerical optimization of the process. In order to model the keyhole growth we proposed a very simple model that adequately serves our purpose.

The results of experimental work show that some theoretically determined laser pulses yield very good results. In some cases we notice a weaker agreement between the theoretical and experimental results, which is the consequence of a relatively simplified theoretical model. However, based on the numerical simulation of the process the experimental results can still be easily understood and interpreted. The theoretical model and optimization procedure are not meant to replace the experimental work completely, but can significantly decrease the extent of the required work. In this manner we should understand the importance of the presented work as being complementary to the experimental work. It allows a faster search for proper parameters and an easier interpretation of experimental results, especially when an important part of the process is changed like the wire material, laser optics, wire-feed system, etc. Though we give a quantitative statistical description of experimental results for the purpose of comparing experimental outcomes, the suitability of the process for a certain application should be determined by the final user in accordance with the specific demands of the application.

Table 1: Quantitative analysis of the experimental outcome for different detachment pulses
Tabela 1: Kvantitativna analiza eksperimentalnih rezultatov za različne ločitvene bliske

P	$\bar{d}$/mm	$\sigma_d/\bar{d}$	$\bar{r}_x$/mm	$\bar{r}_y$/mm	$\bar{r}$/mm	$\sigma_r/\bar{d}$	v	N_{izb}/N_{kap}
8 kW	1.237	0.155	1.024	1.585	1.895	0.355	0.510	100/10 = 10
6 kW	1.223	0.169	−0.008	1.199	1.213	0.155	0.324	48/10 = 4.8
4 kW	1.149	0.098	0.679	1.276	1.458	0.255	0.323	29/8 = 3.6
5 kW	1.111	0.163	0.332	0.843	0.946	0.181	0.344	45/9 = 5

6 REFERENCES

[1] D. Attinger, D. Poulikakos, Melting and resolidification of a substrate caused by molten microdroplet impact, Journal of Heat transfer, 123 (**2001**) 12, 1110–1122

[2] A. M. Ahmed, R. H. Rangel, Metal droplet deposition on non-flat surfaces: effect of surface morphology, International Journal of Heat and Mass Transfer, 45 (**2002**), 1077–1091

[3] S. Cheng, S. Chandra, A pneumatic droplet-on-demand generator, Experiments in fluids, 34 (**2003**), 755–762

[4] J. Brünahl, A. M. Grishin, Piezoelectric shear mode drop-on-demand inkjet actuator, Sensors and Actuators A, 101 (**2002**), 371–382

[5] H. Sohn, D. Y. Yang, Drop on demand deposition of superheated metal droplets for selective infiltration manufacturing, Materials Science and Engineering A, 392 (**2005**) 1–2, 415–421

[6] S. X. Cheng, T. Li, S. Chandra, Producing metal droplets with a pneumatic droplet-on-demand generator, Journal of Materials Processing Technology, 195 (**2005**), 295–302

[7] J. Haidar, An analysis of the formation of metal droplets in arc welding, Journal of Physics D: Applied physics, 31 (**1998**), 1233–1244

[8] E. L. Dreizin, Droplet welding: A new technology for welding electrical contacts, Welding Journal, 76 (**1997**), 67–73

[9] J. J. C. Buelens, Metal droplet deposition: review of innovative joining technique, Science and Technology of Welding and Joining, 6 (**1997**) 2, 239–243

[10] F. Wang, W. K. Hou, S. J. Hu, E. Kannatey-Asibu, W. W. Schultz, P. C. Wang, Modelling and analysis of metal transfer in gas metal arc welding, Journal of Physics D: Applied physics, 36 (**2003**), 1143–1152

[11] W. W. Appelman, Miniaturisation of droplet deposition, Technical report, Philips Centre for Manufacturing Technology, Eindhoven 1995

[12] Y. Wu, R. Kovacevic, Mechanically assisted droplet transfer process in gas metal arc welding, Proceedings of the Institution of Mechanical Engineers, Part B, Journal of engineering manufacture, 216 (**2002**), 555–564

[13] P. P. Conway, E. K. Y. Fu, K. Williams, Precision high temperature lead-free solder interconnections by means of high-energy droplet deposition techniques, CIRP Annals, 51 (**2002**) 1, 177

[14] E. Govekar, B. Jahrsdoerfer, J. Klemenčič, P. Mužič, I. Grabec, Characterization of laser droplet formation process by IR camera images and AE signals, Dynamic Days, Dresden, 2001

[15] W. Hovig, B. Jahrsdorfer, Laser droplet weld - ein innovatives fügeverfahren, Laser in Elektronikproduktion & Feinwerktechnik, LEF 2001, 2001

[16] J. Klemenčič, Investigation of laser droplet formation from thin wire, Master thesis, FS, UL, Ljubljana, 2003

[17] B. Jahrsdorfer, G. Eßer, M. Geiger, E. Govekar, Laser droplet weld – an innovative joining technology opens new application possibilities, Photon Processing in Microelectronics and Photonics II, Proceedings of SPIE, 2003, 4977

[18] E. Govekar, J. Klemenčič, T. Kokalj, B. Jahrsdorfer, P. Mužič, I. Grabec, Characterization of laser droplet formation process by acoustic emission, Ultrasonics, 42 (**2004**), 99–103

[19] B. Jahrsdorfer, M. Schmidt, M. Geiger, Laser droplet welding and its potential for joining dissimilar materials, Laser Assisted Net Shape Engineering 4, Proceedings of LANE 2004, 2004

[20] B. Krese, M. Perc, E. Govekar, The dynamics of laser droplet generation, Chaos, 20 (**2010**), 013129

[21] A. Jerič, I. Grabec, E. Govekar, Laser droplet welding of zinc coated steel sheets, Science and Technology of Welding and Joining, 14 (**2009**) 4, 362–368

[22] T. Kokalj, J. Klemenčič, P. Mužič, I. Grabec, E. Govekar, Analysis of the laser droplet formation process, Journal of Manufacturing Science and Engineering, 128 (**2006**) 1, 307–314

[23] J. W. Thomas, Numerical Partial Differential Equations: Finite Difference Methods, Springer-Verlag, New York 1995

[24] D. Whitley, A genetic algorithm tutorial, Statistics and Computing, 4 (**1994**), 65–85

[25] K. F. Man, K. S. Tang, S. Kwong, Genetic algorithms: Concepts and applications, IEEE Transactions on Industrial Electronics, 5 (**1996**) 43, 519–534

[26] A. E. Eiben, J. E. Smith, Introduction to Evolutionary Computing, Springer, Berlin 2003